Iranian Journal of Basic Medical Sciences
ijbms.mums.ac.ir

An *in vivo* evaluation of the antifibrotic potential of inulin against bile duct ligation-induced liver fibrosis

Yasaman Habibian-Fard [1], Mahsa Ale-Ebrahim [2]*, Parvaneh Mohseni-Moghaddam [2], Shadi Sarahroodi [1], Pejman Mortazavi [3]

[1] Department of Pharmacology and Toxicology, Faculty of Pharmacy and Pharmaceutical Sciences, Tehran Medical Sciences, Islamic Azad University, Tehran, Iran
[2] Department of Physiology, Faculty of Medicine, Tehran Medical Sciences, Islamic Azad University, Tehran, Iran
[3] Department of Pathology, Faculty of Specialized Veterinary Science and Research Branch, Islamic Azad University, Tehran, Iran

ARTICLE INFO

Article type:
Original

Article history:
Received: May 11, 2025
Accepted: Nov 15, 2025

Keywords:
α-actins smooth muscle
Anti-oxidants
Bile duct ligation
Cholestasis
Farnesoid X receptor
Factor-β1
Inulin
Liver fibrosis
Transforming growth

ABSTRACT

Objective(s): Hepatic fibrosis is a major cause of liver-related mortality worldwide. This study evaluated the hepatoprotective and antifibrotic effects of inulin, a natural polysaccharide, in a rat model of cholestasis induced by bile duct ligation (BDL).

Materials and Methods: Thirty male Wistar rats (230–250 g) were randomly divided into six groups: control, sham, inulin (200 mg/kg), BDL, and BDL+ inulin (100 and 200 mg/kg). Inulin was orally administered for 30 days after BDL. Serum liver enzyme levels, bilirubin, and lipid profiles were measured. Liver tissues were analyzed for oxidative stress markers (GPx, MDA), fibrogenic mediators (TGF-β1, α-SMA) via immunohistochemistry and FXR levels by ELISA. Histological changes were evaluated by ELISA and Masson's trichrome staining.

Results: At 200 mg/kg, inulin significantly reversed the BDL-induced increases in serum liver enzymes (AST, ALT, and ALP), total bilirubin, and cholesterol ($P<0.001$ vs BDL group). Hepatic GPx and FXR levels were significantly increased ($P<0.001$ vs BDL group), while MDA levels were decreased ($P<0.001$ vs BDL group). Inulin markedly suppressed the expression of TGF-β1 and α-SMA ($P<0.01$ vs BDL group). Histopathological evaluation showed notable improvement in liver architecture, with reduced fibrosis and necrosis ($P<0.001$ vs BDL group).

Conclusion: These findings suggest that inulin may exert antifibrotic effects through its anti-oxidant activity, ultimately reducing the expression of fibrogenic markers. This study presents strong histological evidence to support the hepatoprotective role of inulin.

▶ Please cite this article as:
Habibian-Fard Y, Ale-Ebrahim M, Mohseni-Moghaddam P, Sarahroodi Sh, Mortazavi P. An *in vivo* evaluation of the antifibrotic potential of inulin against bile duct ligation-induced liver fibrosis. Iran J Basic Med Sci 2026; 29:

Introduction

The liver plays a vital role in the metabolism of nutrients and xenobiotics. Common liver disorders include viral hepatitis, fatty liver disease, and cholestatic fibrosis (1). Liver fibrosis involves excessive extracellular matrix (ECM) accumulation, which disrupts liver function (2). In cholestasis, toxic bile acids induce oxidative stress by generating reactive oxygen species (ROS) and activate hepatic stellate cells (HSC_s), leading to inflammation and fibrosis (3, 4). Oxidative stress promotes lipid peroxidation and synthesis of pro-inflammatory cytokines, further activating HSC_s (5, 6). Anti-oxidants have been shown to inhibit lipid peroxidation and fibrosis (7, 8). Collagen production in the liver is triggered by the transforming growth factor-β (TGF) pathway, which is activated by free radicals (9). TGF-β promotes ECM accumulation and fibrosis by inducing collagen and fibronectin synthesis (10, 11) and inhibiting ECM degradation via overexpression of plasminogen activator inhibitor 1 (PAI-1) (12). TGF-β binds to its receptor, activating receptor-regulated Smads (R-Smads), which form complexes to regulate gene transcription (13). Farnesoid X receptor (FXR), a bile acid-activated nuclear receptor, is activated mainly by bile acid and is expressed in the liver, regulating bile acid homeostasis (14). FXR plays a critical role in maintaining bile acid metabolic homeostasis (15). FXR activation reduces liver fibrosis by inhibiting TGF-β1 secretion, ECM deposition, and inflammation by suppressing markers such as nuclear factor-kappa B (NF-κB) (14).

The management of cholestatic liver fibrosis requires novel compounds with fewer side effects than synthetic drugs. Inulin, a natural β-D-fructan polysaccharide from various plants, is biocompatible and widely used in pharmaceutical and food industries (16, 17). It benefits metabolic syndrome-related diseases such as type 2 diabetes, obesity, fatty liver disease, and dyslipidemia (18). The hepatoprotective effects of inulin have been demonstrated

***Corresponding author:** Mahsa Ale-Ebrahim. Islamic Azad University of Medical Sciences, Shariati St. Tehran, Iran. Email: mahsa.alebrahim@yahoo.com; Aleebrahim@iaups.ac.ir

in methotrexate and carbon tetrachloride (CCl4) models, attributed to its anti-apoptotic, anti-oxidant, and anti-inflammatory properties (17, 19). Inulin also improves liver injury and steatosis induced by high-fat and high-sucrose diets, possibly by suppressing hepatic cytochrome P450 and hepatocyte nuclear factor 4α expression (20). However, its effect on BDL-induced hepatic fibrosis remains unclear. This study evaluated the hepatoprotective, anti-oxidant, and antifibrotic effects of inulin in a BDL model by measuring liver function, lipid profile, FXR expression, and fibrosis markers TGF-β and α-SMA.

Materials and Methods

Animals

A total of 30 male Wistar rats (230–280 g) with free access to tap water and standard pellets were used in this study. The animals were maintained on 12:12 hr light/dark cycles. The protocols used for animal studies were based on the Guide for the Care and Use of Laboratory Animals (National Institutes of Health, USA). Ethical approval for animal experiments was obtained from the Animal Ethics Committee of Tehran Medical Sciences, Islamic Azad University, Tehran, Iran (approval no. IR.IAU.PS.REC.1402.134).

BDL surgery and experimental procedures

All rats were randomly divided into one of the following groups (n=5): (1) the control group receiving 1 milliliter (ml) of inulin solvent, distilled water (DW), for 30 days, once a day; (2) the control + 200: in this group, rats received inulin at the dose of 200 mg/kg orally per day in a period of 30 days; (3) the sham group: in this group, rats with laparotomy and without BDL surgery were administered 1 ml of DW once a day during 30 days; (4) the BDL group: rats underwent BDL surgery and received daily administration of 1 ml of DW for 30 days; (5 and 6) The BDL + 100 and BDL + 200 groups: in these groups, animals with BDL surgery were given oral administration of inulin at doses of 100 and 200 mg/kg, respectively. After inulin was dissolved in its solvent, DW, 1 mL was administered orally to the animals once a day for 30 days. Administration of inulin was commenced on the same day as the BDL surgery was performed. The appropriate doses were chosen according to previously published studies (17, 19). Based on a standard protocol, the BDL surgery was performed (21). First, animals were anesthetized by injection of ketamine (90 mg/kg) and xylazine (10 mg/kg) into the peritoneum. Subsequent to the incision of the abdominal midline and distinguishing the common bile duct, it was ligated in two parts, namely, before the pancreatic duct entrance and below the hepatic duct junction. Afterward, between the two closed areas, the common bile duct was incised. Then, following the addition of 2 mL of sterile saline into the peritoneum, the incision made in the abdomen was stitched. Finally, the animals were put on a heating pad to recover (22). In the case of animals in the sham group, only the abdomen was incised, but BDL was not performed.

Compounds

Inulin was purchased from Alfa Aesar, USA. Commercial kits for measuring total bilirubin, alanine aminotransferase (ALT), alkaline phosphatase (ALP), aspartate aminotransferase (AST), triglyceride, and cholesterol were purchased from Pars Azmoon Company, Iran. The assay kits for activity assessment of glutathione peroxidase (GPx) and liver malondialdehyde (MDA) level were procured from Navand Salamat Company (Iran) and Teb Pazhouhan Razi (Iran), respectively. The Elisa assay kit for FXR was provided by Abbexa Company, UK. TGF-β1 and α-SMA were evaluated using IHC kits obtained from Abcam, UK.

Sampling and biochemical evaluations

The rats underwent an 18-hr fast after completing the animal experiments. The whole liver of the animals and blood samples were extracted after each animal was given a combination of ketamine (90 mg/kg) and xylazine (10 mg/kg) to induce anesthesia. Subsequently, a ketamine and xylazine overdose was used to euthanize each rat. For histological evaluation, a piece of liver tissue was immediately fixed in 10% formaldehyde. An additional piece of liver tissue was homogenized to assess GPx activity, MDA levels, and FXR protein levels.

In order to prepare the serum, animal blood samples were collected and then kept for half an hour at room temperature. They were then centrifuged at 1000 × g for 10 min at 37 °C. Using commercial kits, the following parameters were measured in serum: triglycerides, cholesterol, AST, ALT, ALP, and total bilirubin (23, 24).

Determining the activity of GPx and MDA levels in liver tissue

The glutathione peroxidase (GPx) assay kit was utilized to determine the GPx activity in liver homogenate. In this method, GPx reduces cumene hydroperoxide by first oxidizing GSH to GSSG. Next, GSSG is reduced to GSH by glutathione reductase enzyme using NADPH. In this reaction, the amount of consumed NADPH is used as a marker to estimate GPx activity, which was measured at 340 nm.

The MDA level, an indicator of oxidative stress, was measured using the commercial kit R (Teb Pazhouhan Razi, Tehran, Iran) according to the manufacturer's protocol. Briefly, in this method, MDA in the samples reacted with thiobarbituric acid (TBA). Then, tubes were incubated in boiling water for 1 hr. Subsequently, the cooled tubes underwent centrifugation for a duration of 10 minutes at a speed of 10000 × g at 4 °C, followed by measuring the absorbance at 532 nm.

Assessment of hepatic levels of FXR

With the particular primary antibody and HRP-conjugated secondary antibody acquired from Abbexa Company, UK, the FXR level was assessed in the liver using the sandwich ELISA technique. The final findings were displayed as ng/ml protein.

Histopathological examination

To detect the histopathological changes, such as bile-duct hyperplasia, inflammation, necrosis, and fibrosis, MT staining was employed. Each sample received a single score based on the average of 10 random fields per slide (25). The following scoring system was used to determine the degree of liver damage: necrosis: no necrosis is defined by score 0; focal necrosis in less than 25% of the liver is determined by score 1; focal necrosis in 25% to 50% of the liver is shown by score 2; extensive but focal necrosis is indicated by score 3; and global hepatocyte necrosis is demonstrated by score 4. Fibrosis: 0 for none; 1 for portal fibrosis; 2 for septal formation; 3 for prominent bridging fibrosis; and 4 for cirrhosis. Hyperplasia of the biliary ducts: 0 illustrates none; 1 illustrates hyperplasia in less than 25% of each lobule of the liver; 2 illustrates hyperplasia in 25 to 50% of each lobule of the liver; 3 illustrates extensive but focal hyperplasia of the biliary ducts; and 4 illustrates global ductal hyperplasia.

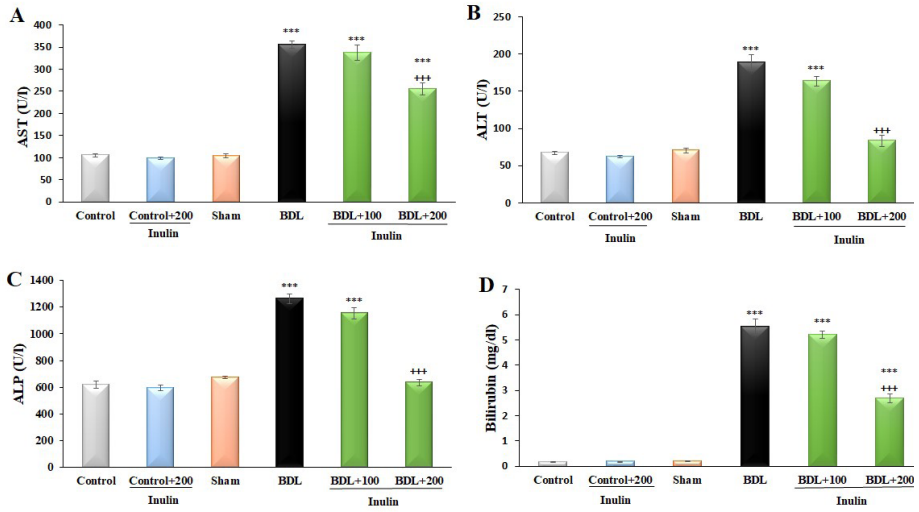

Figure 1. Evaluating the differences in the serum concentrations of the rat liver indices in the experimental groups such as AST (A), ALT (B), ALP (C), and total bilirubin (D)
The serum AST, ALT, ALP, and total bilirubin levels in BDL animals were considerably reduced by inulin at 200 mg/kg. ***P<0.001 versus the sham group, +++P<0.001 compared with the BDL group (n= 5). AST: Aspartate aminotransferase; ALT: Alanine aminotransferase; ALP: Alkaline phosphatase; BDL: Bile duct ligation.

Inflammation: 0 represents no inflammation; 1 represents focal inflammation in less than 25% of the liver; 2 represents focal inflammation in 25% to 50% of the liver; 3 represents extensive but focal inflammation; and 4 represents global inflammation (26).

Immunohistochemistry (IHC) staining

Using the IHC technique, liver expressions of TGF-β1 and α-SMA proteins were assessed. Concisely, a graded alcohol series was used to hydrate deparaffinized liver sections. Following BSA blocking, the sections were incubated overnight at 4 °C with the TGF-β1 and α-SMA primary antibodies (1:100 dilution). The slides were then rinsed with TBS and left at room temperature for an hou while the secondary antibody was incubated. The DAB (3,3′-diaminobenzidine) chromogen was used to assess immunoreactivity. IHC images were evaluated using a Olympus BX43 light microscope (Hamburg, Germany). The expression of TGF-β1 was determined consistently with the positive cells' percentage and scored as follows: Negative TGF-β1 expression (score 0) occurs when the proportion of positive cells in total cells is less than 10%; 10-25%, TGF-β1 expression is weak (score 1); 26-50%, TGF-β1 is moderately expressed (score 2); 51-75% a higher level of TGF- β1 expression (score 3); and levels above 75% are the highest level of TGF- β1 expression (score 4). Additionally, based on the percentage of positive cells, the liver α-SMA expression was assessed and categorized as follows: expression of α-SMA in < 3% of cells (score 0); α-SMA expression in 3–33% of cells (score 1); expression of α-SMA in 34–66% of cells (score 2); and α-SMA expression in more than 66% of cells (score 3).

Statistical analyses

Mean ± SEM was used to present the data. To examine the statistical variances among the experimental groups, a one-way ANOVA and a Tukey *post hoc* test were applied. SPSS software (version 24) was utilized to perform data analysis. Statistics were considered significant when the *P*-value was <0.05.

Results

Biochemical analysis

Based on Figure 1, compared with the sham group, BDL significantly increased serum biomarkers of liver injury, including AST, ALT, and ALP (P<0.001 for all variables). After receiving a dose of 200 mg/kg of inulin, the elevated liver levels of AST, ALT, and ALP in the BDL animals were significantly reduced (P<0.001 for all variables). As demonstrated in Figure 1, the animals undergoing BDL surgery had significantly higher serum total bilirubin levels (P<0.001) than the sham group. When inulin at a dose of 200 mg/kg was administered to BDL animals, the serum total bilirubin level was significantly reduced (P<0.001). Moreover, compared with the sham group, BDL significantly increased serum cholesterol levels (P<0.001), while it did not alter serum triglyceride levels substantially. Comparing the BDL group to the inulin-treated group, Figure 2 illustrates that administering inulin at a dose of 200

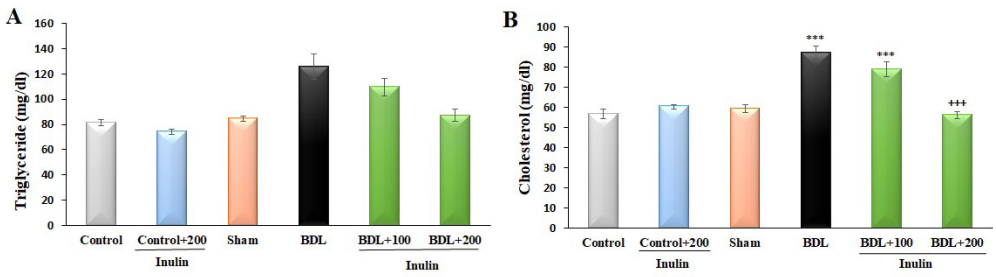

Figure 2. Triglyceride (A) and cholesterol (B) levels in the serum of rats
At 200 mg/kg, inulin could markedly lower the serum cholesterol level in BDL animals. ***P<0.001 versus the sham group, +++P<0.001 in contrast to the BDL group (n= 5). BDL: Bile duct ligation.

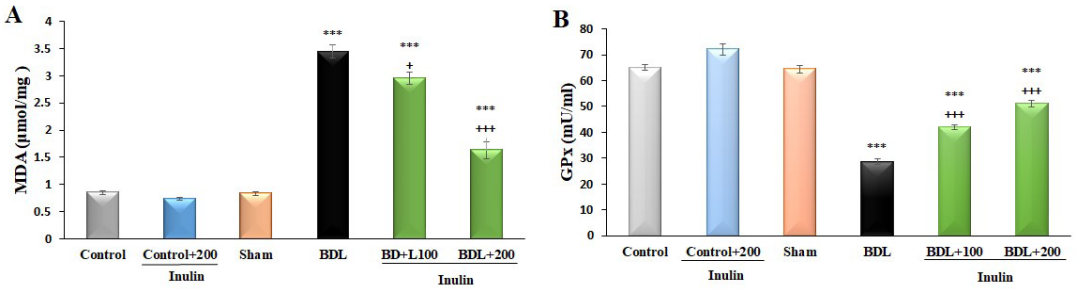

Figure 3. Evaluating the rat liver levels of MDA (A) and liver GPx activity (B)100 and 200 mg/kg of inulin significantly decreased MDA level in the animals undergoing BDL surgery Both doses of inulin could also increase the GPx activity. ***P<0.001 in contrast to the sham group, +P<0.05 and +++P<0.001 compared with the BDL group (n= 5). BDL: Bile duct ligation; GPx: Glutathione peroxidase; MDA: Malondialdehyde.

mg/kg considerably reduced the serum cholesterol levels.

The liver of the BDL group showed significantly higher MDA levels and lower GPx activity compared with the sham group, as shown in Figures 3A and 3 B (P<0.001 for both variables). When 100 and 200 mg/kg of inulin were administered to animals that had undergone BDL surgery, there was a significant reduction in MDA levels (P<0.05 and P<0.001, respectively) compared with the BDL group; in addition, GPx activity increased (P<0.001 for both doses). Furthermore, no statistically significant variations were observed in the levels of the aforementioned investigated parameters among the three groups: the control group, the inulin-treated control group, and the sham group. According to the findings, the 200 mg/kg dose was the most effective for lowering hepatic indices, modifying lipid profiles, and increasing anti-oxidant potential.

Inulin improved liver fibrosis

Results indicate that the BDL group had significantly higher histological scores for liver injury than the sham group did. Additionally, the livers of BDL animals treated with inulin at 100 and 200 mg/kg showed a significant improvement in histopathologic scores (Table 1). Hepatocyte necrosis, ductal hyperplasia, collagen deposition, and lymphocyte infiltration—all indicators of liver fibrosis—were seen in the BDL animals according to histological data derived from MT staining. The fibrosis indices, as mentioned earlier, were markedly decreased in BDL animals fed with inulin at doses of 100 and 200 mg/kg. Furthermore, compared with the control group, no histological abnormalities were found in the livers of the sham group or the control + inulin group. Hepatocytes, bile ducts, and the portal tract were all intact, indicating normal liver histology (Figure 4). In the control, sham,

Table 1. Rat hepatic injury score

	Control	Control+200 mg/kg inulin	Sham	BDL	BDL+ 100 mg/kg inulin	BDL+ 200 mg/kg inulin
Necrosis	0	0	0	3.06+ 0.20***	2.03+0.11++	1.11+0.40+++
Inflammation	0	0	0	3.70+ 0.18***	2.00+0.10+++	1.00+0.12+++
Collagen deposition	0	0	0	3.81+ 0.11***	1.98+1.00+++	1.96+0.11+++
Ductal hyperplasia	0	0	0	3.64+0.10***	1.91+0.21+++	0.98+0.02+++

***P<0.001 versus the sham group, ++P<0.01 and +++P<0.001 in contrast to the BDL group. BDL: Bile duct ligation

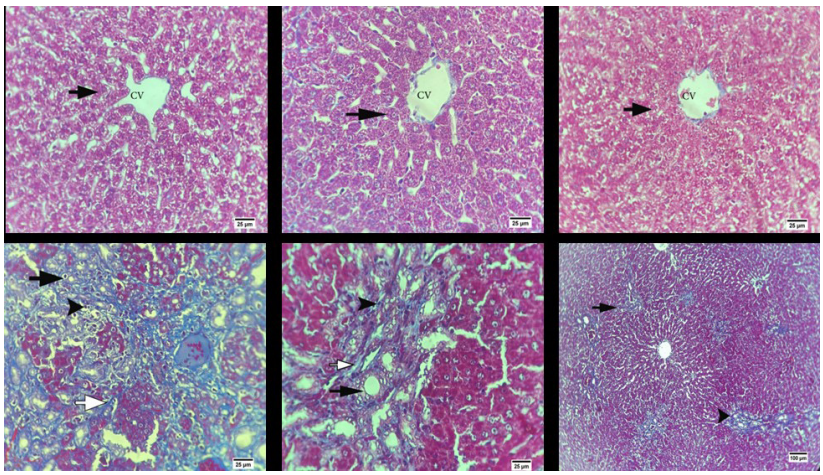

Figure 4. Rat hepatic fibrosis assessment through MT staining
(A) Control (×400, MT staining), (B) Control + inulin at the dose of 200 mg/kg (×400, MT staining), (C) Sham (×400, MT staining), (D) BDL (×400, MT staining), (E) BDL + inulin at the dose of 100 mg/kg (×400, MT staining), and (F) BDL + inulin at the dose of 200 mg/kg (×400, MT staining)
The hepatic tissue in the control, control + inulin group, and sham group (A and B) showed no histological abnormalities, and the hepatocytes (arrowheads) surrounding the CV, as well as the CV, were normal. The liver of the BDL group showed signs of widespread bridging fibrosis (arrow) and ductal hyperplasia (arrowheads) (D). Treatment with inulin markedly improved liver fibrosis (E and F).
BDL: Bile duct ligation; CV: Central vein; MT: Masson trichrome

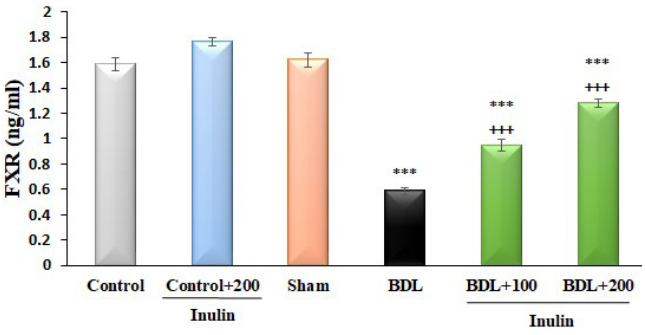

Figure 5. ELISA evaluation of rat FXR protein
100 and 200 mg/kg of inulin significantly augmented the FXR expression in the animals undergoing BDL surgery. ***P<0.001 in contrast to the sham group, +++P<0.001 compared with the BDL group (n= 5). BDL: Bile duct ligation; FXR: Farnesoid X receptor.

and inulin 200 mg/kg groups, the liver sections exhibited normal lobular architecture without necrosis, inflammation, fibrosis, or bile ductular hyperplasia, consistent with the morphology of healthy rat livers. Therefore, the histological parameters in these groups received a score of 0, consistent with expected normal tissue features.

All histological images were obtained from comparable lobular regions across all experimental groups. Although the periportal areas in the BDL and treatment groups may appear different due to ductular proliferation, these structures represent proliferated bile ducts replacing necrotic hepatocytes rather than the true portal tracts. Thus, equivalent hepatic regions were used for histopathological comparisons.

Inulin increased the expression of FXR in the liver tissue of animals with BDL surgery

The ELISA assay was used to quantify FXR expression. Compared to the sham group, BDL surgery resulted in a significant decrease in the liver FXR content (P<0.001). In comparison to the BDL group, our findings demonstrated that the FXR content increased in BDL animals when inulin (at both doses) was used (P<0.001) (Figure 5).

Inulin attenuated liver expressions of TGF-β1 and α-SMA proteins in BDL animals

The control group, the inulin-consuming control group, and the sham group did not exhibit TGF-β1 expression in hepatocytes surrounding the central vein (CV) or in other hepatocytes (Figure 6). On the other hand, elevated TGF-β1 levels were observed in the hepatocytes of the BDL group. Comparing the BDL group with the treatment groups, the administration of inulin at the high dose (200 mg/kg) significantly decreased the expression of TGF-β1 (P<0.01) (Figure 6 and Table 2).

According to the information presented in Figure 7 and Table 3, histopathological evaluation revealed no α-SMA expression in the control, inulin-fed control, and sham groups. Conversely, the BDL group exhibited a significant α-SMA expression in both hepatocyte cells and hyperplastic biliary ducts. When comparing the treatment groups with the BDL group, inulin at the high dose significantly decreased α-SMA expression (P<0.01).

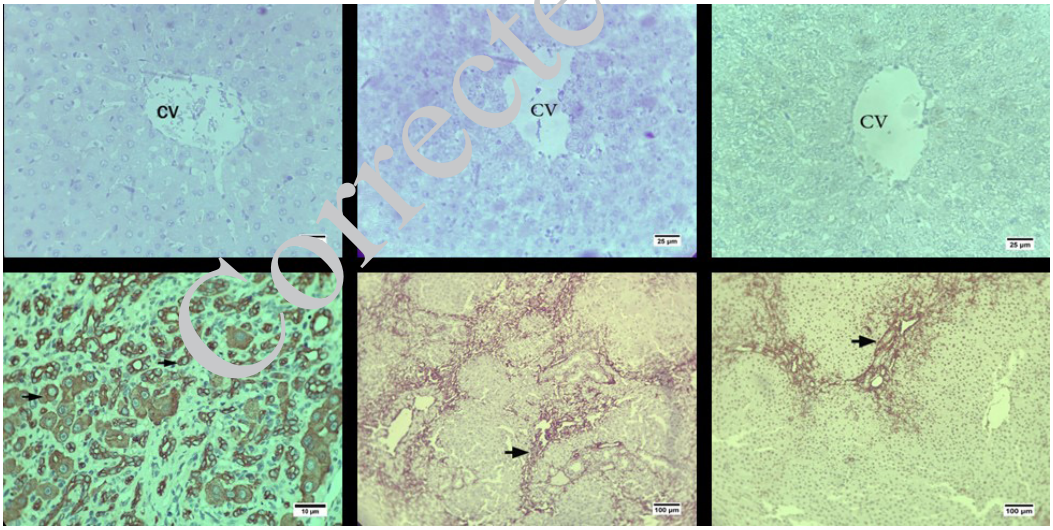

Figure 6. IHC evaluation of (×400) TGF-β1 expression in rat groups
(A) control group, (B) control + 200 mg/kg inulin, (C) sham group, (D) BDL, (E) BDL + 100 mg/kg inulin, and (F) BDL + 200 mg/kg inulin. Protein expression of TGF-β1 in liver fibrosis induced by BDL was reduced by inulin at the dose of 200 mg/kg. Expression of TGF-β1 in hepatic tissue is demonstrated by brown staining, as shown by arrowheads. BDL: Bile duct ligation; CV: Central vein; TGF-β: Transforming growth factor-β1; IHC: Immunohistochemistry

Table 2. Comparing the expression of TGF-β1 in hepatic tissues among various rat groups

Groups	Control	Control+200 mg/kg inulin	Sham	BDL	BDL+ 100 mg/kg inulin	BDL+ 200 mg/kg inulin
Score of TGF-β1 expression	0	0	0	3.31± 0.11***	2.99± 0.29	2.00± 0.21++

The symbol *** denotes a significant difference (P<0.001) when compared to the sham group, whereas ++ indicates significant differences (P<0.01) in relation to the BDL model. BDL: Bile duct ligation; TGF-β: Transforming growth factor-β1

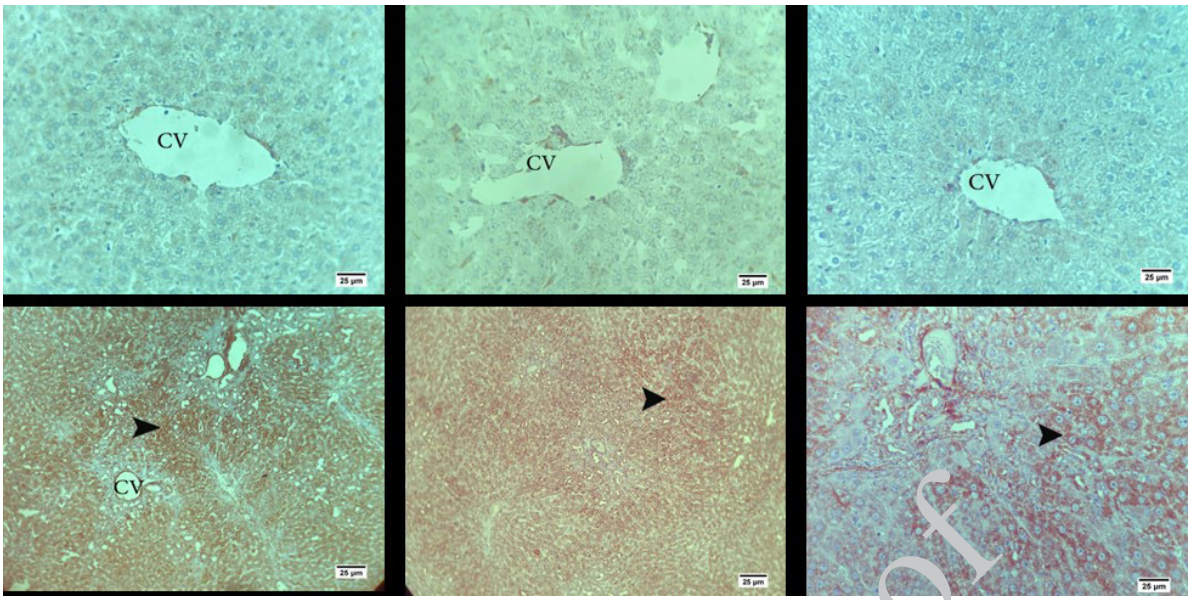

Figure 7. IHC evaluation of (×400) α-SMA expression in rats
(A) control group, (B) control + 200 mg/kg inulin, (C) sham group, (D) BDL, (E) BDL + 100 mg/kg inulin, and (F) BDL + 200 mg/kg inulin. Protein expression of α-SMA in liver fibrosis induced by BDL was reduced by inulin at the dose of 200 mg/kg. Expression of α-SMA in hepatic tissues is demonstrated by brown staining, as shown by arrowheads. α-SMA: Alpha-smooth muscle actin; BDL: Bile duct ligation; CV: Central vein.

Table 3. Comparing the expression of Alpha-smooth muscle actin (α-SMA) in hepatic tissues among various rat groups

Groups	Control	Control+200 mg/kg inulin	Sham	BDL	BDL+ 100 mg/kg inulin	BDL+ 200 mg/kg inulin
Score of α-SMA expression	0	0	0	2.97± 0.11***	2.83± 0.33	2.02± 0.12++

The symbol *** denotes a significant difference (P<0.001) when compared to the sham group, whereas ++ indicates significant differences (P<0.01) in relation to the BDL model. BDL: Bile duct ligation

Discussion

The present investigation assessed the anti-fibrotic and hepatoprotective effects of inulin in BDL-induced liver fibrosis. Serum ALT, ALP, and AST levels were measured to indirectly assess liver status. In response to BDL, serum ALT, ALP, and AST levels were increased significantly. Detergent effects of bile acids on lipid molecules appear to be what promotes the disruption of cell membranes (27). Additionally, specific alterations in lipids, proteins, and nucleic acids are brought about by bile acid accumulation-induced production of ROS, which ultimately damages hepatocyte cells (28). As a result, the bloodstream is exposed to high concentrations of ALP, ALT, and AST released by damaged hepatocytes (29-31). When inulin was given to BDL rats, we observed significant reductions in serum AST, ALT, and ALP. This aligns with previous animal studies (19, 32-34) that also showed reductions in hepatic enzymes after inulin treatment. For example, in a murine NAFLD model, inulin modulated gut microbiota and inhibited TLR4/NF-κB/NLRP3 signaling, leading to lower ALT and improved liver enzymes (33, 34). Moreover, a clinical study in NAFLD patients found that ALT levels decreased following inulin supplementation, which was linked to restoring microbiota balance (35).

Another parameter in this study whose serum level increased following BDL surgery was total bilirubin. A rise in serum total bilirubin levels is the main indicator of cholestasis. Conjugated bilirubin would efflux back into the circulation due to decreased excretion into the bile subsequent to cholestasis. Bilirubin appears to regurgitate into the bloodstream due to compromised tight junctions between hepatocytes (36). Oral inulin administration could potentially lower serum total bilirubin levels in animals with BDL, demonstrating the anti-oxidant properties and its ability to preserve cellular membrane integrity.

Lipid peroxidation and oxidative stress are indicated by the accumulated MDA in tissues. Lipid peroxidation impairs membrane integrity, alters permeability and fluidity, disrupts ion transport, and inhibits metabolic activity (37, 38). This oxidative stress biomarker, MDA, has previously been reported to be elevated in the BDL model (38, 39), findings that are also consistent with our results. Anti-oxidant enzymes, such as catalase, superoxide dismutase (SOD), and GPx, can protect cellular constituents from ROS-induced damage (39). GPx is an essential enzyme that catalyzes hydrogen peroxide reduction (38). The amount of this enzyme decreases in animals that have undergone BDL surgery (39), as observed in our study. Our observation that inulin lowers MDA and enhances GP_x activity in BDL animals is consistent with earlier reports (19, 32, 40). For instance, Kalantari *et al.* reported similar anti-oxidant effects in CCl4-induced hepatic injury (19), and others confirmed these in different liver damage models. (32, 40). Feeding mice an inulin-based diet increased Bacteroidetes levels in their gut microbiota. This, in turn, resulted in a notable rise in short-chain fatty acids (SCFAs) in the portal vein of the animals. Propionic acid showed the highest increase among the SCFAs. Notably, inulin-induced propionic acid played a crucial role in mitigating liver ischemia-reperfusion injury. It exerted anti-oxidative and anti-inflammatory effects,

effectively suppressing ischemia-reperfusion-induced liver cell death (41).

Significant alterations in the lipid profile and hyperlipidemia are concomitant with cholestasis. A decrease in serum HDL levels and increases in serum LDL and total cholesterol levels occur following cholestasis and bile duct obstruction (42, 43). High serum cholesterol and hypercholesterolemia are caused by abnormalities in the removal of cholesterol and bile salts from the body (44). Furthermore, after cholestasis, 3-hydroxy-3-methylglutaryl-coenzyme A (HMG-CoA) reductase activity increases, thereby increasing hepatic cholesterol synthesis. A number of transporters that carry cholesterol from the liver to the blood are overexpressed during cholestasis (45). The primary protein component of HDL, apolipoprotein AI (apoA-I), is less synthesized in cholestasis, thereby lowering HDL levels in serum (46). The research has also shown that chronic inflammation boosts lipid metabolism abnormalities, leading to steatosis and steatohepatitis (34). According to the current study, inulin could lower serum cholesterol levels in BDL animals. This finding is consistent with other studies using different animal models (33, 47). In NAFLD, inulin increased beneficial bacteria in the gut microbiota, leading to reduced liver damage and modulation of the lipid profile (33). The findings of a study revealed that synthetic inulin effectively decreases liver triglycerides and cholesterol levels when compared to a cafeteria diet group. The livers of rats fed the cafeteria diet exhibited increased mRNA levels of fatty acid synthase and acetyl-CoA carboxylase, both of which play roles in regulating de novo lipogenesis. However, dietary inulin resulted in a reduction of the mRNA levels of fatty acid synthase and acetyl-CoA carboxylase synthase. Consequently, this led to the inhibition of liver synthesis of fatty acids. Inulin intake decreases the transcription factors sterol regulatory element-binding protein 1 (SREBP1) and carbohydrate-responsive element-binding protein (ChREBP), which activate genes necessary for fatty acid synthesis (47).

Additionally, the current investigation demonstrated that inulin significantly attenuated histologic abnormalities, including collagen deposition, ductal hyperplasia, hepatocellular necrosis, and inflammatory cell infiltration (Table 1). Hepatic H&E assay also previously indicated that inulin had a significant positive impact on alcoholic steatohepatitis by modulating gut microbiota dysbiosis and inhibiting inflammation (34).

Activation of FXR signaling, triggered by bile acids in the intestine and liver, has been shown to have anti-inflammatory effects in macrophages, intestines, and hepatocytes. This is achieved by inhibiting NF-κB translocation to the nucleus and by counteracting the induction of NF-κB-dependent pro-inflammatory cytokines (48, 49). Additionally, FXR plays a direct role in lipid metabolism. It reduces the expression of SREBP-1 and ChREBP, which are essential for lipogenesis (50), and enhances lipoprotein lipase (LPL) activity (51). Activation of FXR led to a reduction in renal Smad3 levels. Smad3 is an essential molecule that enhances collagen production and thus facilitates the development of fibrosis (52). We found that inulin significantly upregulated FXR in BDL rats, corroborating the findings of Wang *et al.* (53). Studies with FXR agonists, such as obeticholic acid, have demonstrated reductions in TGF-β1 levels, HSC activation, and fibrosis in models of toxic cirrhosis (54). These findings suggest that FXR modulation is a plausible mechanism in our model. TGF-β plays a crucial role in activating HSCs, which ultimately leads to the accumulation of ECM and the development of fibrosis (10, 11). BAR704 is an FXR agonist with selective activity that effectively inhibits liver fibrosis by disrupting the TGFβ-Smad3 signaling in HSCs (54). Research has shown that inulin significantly reduced α-SMA expression, thereby preventing colonic fibrosis induced by irradiation *in vivo* (55).

Inulin reduced oxidative stress and the expression of TGF-β1 and α-SMA, according to the results of this study. Prior studies have documented a reciprocal relationship between ROS and the TGF-β1 pathway (9). ROS can activate the TGF-β1 signaling pathway. Following that, TGF-β1 triggers various pathways, including Smad-dependent and Smad-independent pathways (e.g., c-Jun N-terminal kinases (JNK) and PI3K) (56). Profibrotic genes like COL1, α-SMA, and NADPH oxidase (NOX4) are transcriptionally induced by activated TGF-β1 signaling. Increased NOX4 expression leads to increased ROS production. In addition to activating JNK and NF-κB (9, 57, 58), ROS also increases the oxidation of DNA bases, causing irreversible damage. The combination of these events promotes myofibroblast development and excessive ECM deposition, ultimately leading to fibrosis (9). The current investigation suggests that inulin may have hindered the progression of liver fibrosis by reducing oxidative stress and increasing FXR expression, thereby inhibiting TGF-β1 signaling.

Conclusion

BDL surgery considerably raised liver enzymes and altered the lipid profile. In addition to detecting histological abnormalities, liver anti-oxidant activity was decreased following BDL surgery. TGF-β1 and α-SMA expression was also augmented following BDL, while FXR level was reduced. In inulin-fed animals, biochemical variables were significantly restored. The findings demonstrate that inulin prevented and ameliorated cholestatic liver fibrosis, potentially by lowering oxidative stress, increasing FXR expression, and ultimately preventing the TGF-β1 pathway.

Acknowledgment

The results presented in this paper were part of a student's thesis. The student provided financial resources.

Authors' Contributions

Y HF contributed to funding acquisition, investigation, methodology, review, and editing. M AE handled conceptualization, project administration, supervision, formal analysis, and writing—review and editing. P MM was involved in conceptualization, project administration, supervision, formal analysis, and writing—review and editing. S S supervised, performed formal analysis. PM managed methodology and formal analysis. All authors approved the final manuscript. All data were generated in-house, and no paper mill was used. All authors agree to be accountable for all aspects of work, ensuring integrity and accuracy.

Conflicts of Interest

The authors declare that they have no known competing financial interests or personal relationships that could have appeared to influence the work reported in this paper.

Declaration

We acknowledge that Grammarly software was used to

enhance the language and grammar of the manuscript.

References

1. Ingawale DK, Mandlik SK, Naik SR. Models of hepatotoxicity and the underlying cellular, biochemical and immunological mechanism (s): A critical discussion. Environ Toxicol Pharmacol 2014;37:118-133.
2. Yin C, Evason KJ, Asahina K, Stainier DY. Hepatic stellate cells in liver development, regeneration, and cancer. J Clin Invest 2013;123:1902-1910.
3. Chen WY, Chen CJ, Liao JW, Mao FC. Chromium attenuates hepatic damage in a rat model of chronic cholestasis. Life Sci 2009;84:606-614.
4. Cruz A, Padillo FJ, Granados J, Túnez I, Muñoz MC, Briceño J, *et al.* Effect of melatonin on cholestatic oxidative stress under constant light exposure. Cell Biochem Funct 2003; 21:377-380.
5. Yang JH, Kim SC, Kim KM, Jang CH, Cho SS, Kim SJ, *et al.* Isorhamnetin attenuates liver fibrosis by inhibiting TGF-β/Smad signaling and relieving oxidative stress. Eur J Pharmacol 2016;783:92-102.
6. Han JM, Kim HG, Choi MK, Lee JS, Park HJ, Wang JH, *et al.* Aqueous extract of Artemisia iwayomogi Kitamura attenuates cholestatic liver fibrosis in a rat model of bile duct ligation. Food Chem Toxicol 2012;50:3505-3513.
7. Karkhaneh L, Yaghmaei P, Parivar K, Sadeghizadeh M, Ebrahim-Habibi A. Effect of trans-chalcone on atheroma plaque formation, liver fibrosis and adiponectin gene expression in cholesterol-fed NMRI mice. Pharmacol Rep 2016;68:720-727.
8. Singh H, Sidhu S, Chopra K, Khan MU. Hepatoprotective effect of trans-chalcone on experimentally induced hepatic injury in rats: inhibition of hepatic inflammation and fibrosis. Can J Physiol Pharmacol 2016;94:879-887.
9. Morry J, Ngamcherdtrakul W, Yantasee W. Oxidative stress in cancer and fibrosis: Opportunity for therapeutic intervention with antioxidant compounds, enzymes, and nanoparticles. Redox Biol 2017;11:240-253.
10. Casini A, Pinzani M, Milani S, Grappone C, Galli G, Jezequel AM, *et al.* Regulation of extracellular matrix synthesis by transforming growth factor β1 in human fat-storing cells. Gastroenterology 1993;105:245-253.
11. Ramadori G, Knittel T, Odenthal M, Schwögler S, Neubauer K, Zum Büschenfelde KHM. Synthesis of cellular fibronectin by rat liver fat-storing (Ito) cells: Regulation by cytokines. Gastroenterology 1992;103:1313-1321.
12. Sawdey MS, Loskutoff DJ. Regulation of murine type 1 plasminogen activator inhibitor gene expression *in vivo*. Tissue specificity and induction by lipopolysaccharide, tumor necrosis factor-alpha, and transforming growth factor-beta. J Clin Invest 1991;88:1346-1353.
13. Inagaki Y, Okazaki I. Emerging insights into transforming growth factor β Smad signal in hepatic fibrogenesis. Gut. 2007;56:284-292.
14. Adorini L, Trauner M. FXR agonists in NASH treatment. J Hepatol 2023;79:1317-1331.
15. Pan PH, Wang YY, Lin SY, Liao SL, Chen YF, Huang WC, *et al.* Plumbagin ameliorates bile duct ligation-induced cholestatic liver injury in rats. Biomed Pharmacother 2022;151:113133.
16. Apolinário AC, de Lima Damasceno BPG, de Macêdo Beltrão NE, Pessoa A, Converti A, da Silva JA. Inulin-type fructans: A review on different aspects of biochemical and pharmaceutical technology. Carbohydr Polym 2014;101:368-378.
17. Liu J, Lu JF, Wen XY, Kan J, Jin CH. Anti-oxidant and protective effect of inulin and catechin grafted inulin against CCl_4-induced liver injury. Int J Biol Macromol 2015;72:1479-1484.
18. Barbero-Becerra V, Juárez-Hernández E, Chávez-Tapia NC, Uribe M. Inulin as a clinical therapeutic intervention in metabolic associated fatty liver disease. Food Rev Int 2021;38:336-348.
19. Kalantari H, Asadmasjedi N, Abyaz Mr, Mahdavinia M, Mohammadtaghvaei N. Protective effect of inulin on methotrexate-induced liver toxicity in mice. Biomed Pharmacother 2019;110:943-950.
20. Sugatani J, Wada T, Osabe M, Yamakawa K, Yoshinari K, Miwa M. Dietary inulin alleviates hepatic steatosis and xenobiotics-induced liver injury in rats fed a high-fat and high-sucrose diet: Association with the suppression of hepatic cytochrome P450 and hepatocyte nuclear factor 4alpha expression. Drug Metab Dispos 2006;34:1677-1687.
21. Uchinami H, Seki E, Brenner DA, D'Armiento J. Loss of MMP 13 attenuates murine hepatic injury and fibrosis during cholestasis. Hepatol 2006;44:420-429.
22. Gross Jr JB, Reichen J, Zeltner TB, Zimmermann A. The evolution of changes in quantitative liver function tests in a rat model of biliary cirrhosis: Correlation with morphometric measurement of hepatocyte mass. Hepatology 1987;7:457-763.
23. Rifai N. Tietz textbook of clinical chemistry and molecular diagnostics-e-book: Elsevier Health Sci; 2017.
24. Moss D. Clinical enzymology. Nature 1971;233:505-505.
25. Sant'Anna LB, Cargnoni A, Ressel L, Vanosi G, Parolini O. Amniotic membrane application reduces liver fibrosis in a bile duct ligation rat model. Cell Transplant 2011;20:441-453.
26. French SW, Miyamoto K, Ohta Y, Geoffrion Y. Pathogenesis of experimental alcoholic liver disease in the rat. Methods Achiev Exp Pathol 1988;13:181-207.
27. Perez MJ, Briz O. Bile-acid-induced cell injury and protection. World J of Gastroenterol 2009;15:1677-1689.
28. Sokol RJ, Straka MS, Dahl R, Devereaux MW, Yerushalmi B, Gumpricht E, *et al.* Role of oxidant stress in the permeability transition induced in rat hepatic mitochondria by hydrophobic bile acids. Pediatr Res 2001;49:519-531.
29. Ale-Ebrahim M, Eidi A, Mortazavi P, Tavangar SM, Minaei Tehrani D. Hepatoprotective and antifibrotic effects of sodium molybdate in a rat model of bile duct ligation. J Trace Elem Med Biol 2015;29:242-248.
30. Ramaiah SK. A toxicologist guide to the diagnostic interpretation of hepatic biochemical parameters. Food Chem Toxicol 2007;45:1551-1557.
31. Javadi F, Ale-Ebrahim M, Mohseni-Moghaddam P, Mortazavi P, Mousavi Z, Asghari A. Hepatoprotective and antifibrotic effects of trans-chalcone against bile duct ligation-induced liver fibrosis in rats. Iran J Basic Med Sci 2023;26:1194-1201.
32. Du H, Zhao A, Wang Q, Yang X, Ren D. Supplementation of inulin with various degree of polymerization ameliorates liver injury and gut microbiota dysbiosis in high fat-fed obese mice. J Agric Food Chem 2020;68:779-787.
33. Bao T, He F, Zhang X, Zhu L, Wang Z, Lu H, *et al.* Inulin exerts beneficial effects on non-alcoholic fatty liver disease via modulating gut microbiome and suppressing the lipopolysaccharide-toll-like receptor 4-mψ-nuclear factor-κb-nod-like receptor protein 3 pathway via gut-liver axis in mice. Front Pharmacol 2020;11:558525.
34. Yang X, He F, Zhang Y, Xue J, Li K, Zhang X, *et al.* Inulin ameliorates alcoholic liver disease via suppressing LPS-TLR 4-Mψ axis and modulating gut microbiota in mice. Alcohol Clin Exp Res 2019;43:411-424.
35. Chong CYL, Orr D, Plank LD, Vatanen T, O'Sullivan JM, Murphy R. Randomised double-blind placebo-controlled trial of inulin with metronidazole in non-alcoholic fatty liver disease (NAFLD). Nutrients 2020;12:937-951.
36. Trauner M, Meier PJ, Boyer JL. Molecular pathogenesis of cholestasis. N Engl J Med 1998;339:1217-1227.
37. Catalá A. Lipid peroxidation modifies the picture of membranes from the "Fluid Mosaic Model" to the "Lipid Whisker Model". Biochim 2012;94:101-109.
38. Salehi V, Malekiasl H, Azizi M, Nouripour-Sisakht S, Gharaghani M, Saberinejad AA, *et al. Oliveria decumbens* extract exhibits hepatoprotective effects against bile duct ligation-induced liver injury in rats by reducing oxidative stress. Hepat Mon 2023;23: e131160.
39. Sadeghi H, Azarmehr N, Razmkhah F, Sadeghi H, Danaei N, Omidifar N, *et al.* The hydroalcoholic extract of watercress

attenuates protein oxidation, oxidative stress, and liver damage after bile duct ligation in rats. J Cell Biochem 2019;120:14875-14884.
40. Nabil MAH, Hnaa AH, Hanaa MS, Amr MM. A promising chemosesitization role of inulin in management of experimentally induced hepatocellular carcinoma. Iraq Med J 2017;1:83-87.
41. Kawasoe J, Uchida Y, Kawamoto H, Miyauchi T, Watanabe T, Saga K, *et al.* Propionic acid, induced in gut by an inulin diet, suppresses inflammation and ameliorates liver ischemia and reperfusion injury in mice. Front Immunol 2022;13:862503.
42. Ji H, Jiang JY, Xu Z, Kroeger EA, Lee SS, Liu H, *et al.* Change in lipid profile and impairment of endothelium-dependent relaxation of blood vessels in rats after bile duct ligation. Life Sci 2003;73:1253-1263.
43. Longo M, Crosignani A, Podda M. Hyperlipidemia in chronic cholestatic liver disease. Curr Treat Options Gastroenterol 2001;4:111-114.
44. Delgado-Villa MJ, Ojeda ML, Rubio JM, Murillo ML, Sánchez OC. Beneficial role of dietary folic acid on cholesterol and bile acid metabolism in ethanol-fed rats. J Stud Alcohol Drugs 2009;70:615-622.
45. Nuño-Lámbarri N, Barbero-Becerra VJ, Uribe M, Chávez-Tapia NC. Elevated cholesterol levels have a poor prognosis in a cholestasis scenario. J Biochem Mol Toxicol 2017;31:1-6.
46. Claudel T, Sturm E, Duez H, Torra IP, Sirvent A, Kosykh V, *et al.* Bile acid-activated nuclear receptor FXR suppresses apolipoprotein AI transcription via a negative FXR response element. J Clin Invest 2002;109:961-971.
47. Sugatani J, Osabe M, Wada T, Yamakawa K, Yamazaki Y, Takahashi T, *et al.* Comparison of enzymatically synthesized inulin, resistant maltodextrin and clofibrate effects on biomarkers of metabolic disease in rats fed a high-fat and high-sucrose (cafeteria) diet. Eur J Nutr 2008;47:192-200.
48. Hao H, Cao L, Jiang C, Che Y, Zhang S, Takahashi S, *et al.* Farnesoid X receptor regulation of the NLRP3 inflammasome underlies cholestasis-associated sepsis. Cell Metabol 2017;25:856-867.
49. Wang YD, Chen WD, Wang M, Yu D, Forman BM, Huang W. Farnesoid X receptor antagonizes nuclear factor κB in hepatic inflammatory response. Hepatology 2008;48:1632-1643.
50. Khan RS, Bril F, Cusi K, Newsome PN. Modulation of insulin resistance in nonalcoholic fatty liver disease. Hepatology 2019;70:711-724.
51. Chávez-Talavera O, Tailleux A, Lefebvre P, Staels B. Bile acid control of metabolism and inflammation in obesity, type 2 diabetes, dyslipidemia, and nonalcoholic fatty liver disease. Gastroenterology 2017;152:1679-94.
52. Alipour MR, Jeddi S, Karimi-Sales E. Trans-Chalcone inhibits high-fat diet-induced disturbances in FXR/SREBP-1c/FAS and FXR/Smad-3 pathways in the kidney of rats. J Food Biochem 2020;44:e13476.
53. Wang R, Ren Y, Bao T, Wang T, Li Y, Liu Y, *et al.* Inulin activates FXR-FGF15 signaling and further increases bile acids excretion in non-alcoholic fatty liver disease mice. Biochem Biophys Res Commun 2022;600:156-162.
54. Carino A, Biagioli M, Marchianò S, Scarpelli P, Zampella A, Limongelli V, *et al.* Disruption of TFGβ-SMAD3 pathway by the nuclear receptor SHP mediates the antifibrotic activities of BAR704, a novel highly selective FXR ligand. Pharmacol Res 2018;131:17-31.
55. Ji K, Zhang M, Du L, Liu Y, Xu C, He N, *et al.* Targeting the gut microbiota with inulin: a novel approach for the management of irradiation-induced colonic fibrosis. Res Sq 2022;https://doi.org/10.21203/rs.3.rs-139[illegible]
56. Liu RM, Desai LP. Reciprocal regulation of TGF-β and reactive oxygen species: A perverse cycle for fibrosis. Redox Biol 2015;6:565-577.
57. Nakamura H, Nakajima A, Sakon-Komazawa S, Piao JH, Xue X, Okumura K. Reactive oxygen species mediate crosstalk between NF-κB and JNK. Cell Death Differ 2006;13:730-737.
58. Chan EC, Peshavariya HM, Liu GS, Jiang F, Lim SY, Dusting GJ. Nox4 modulates collagen production stimulated by transforming growth factor β1 *in vivo* and *in vitro*. Biochem Biophys Res Commun 2013;430:918-925.